Photoinduced Enhancement of the Charge Density Wave Amplitude

A. Singer,[1,*] S. K. K. Patel,[1,2] R. Kukreja,[1,2] V. Uhlíř,[2] J. Wingert,[1] S. Festersen,[3] D. Zhu,[4]
J. M. Glownia,[4] H. T. Lemke,[4,†] S. Nelson,[4] M. Kozina,[4] K. Rossnagel,[3] M. Bauer,[3] B. M. Murphy,[5,3]
O. M. Magnussen,[3,5] E. E. Fullerton,[2] and O. G. Shpyrko[1]

[1]*Department of Physics, University of California–San Diego, La Jolla, California 92093, USA*
[2]*Center for Memory and Recording Research, University of California–San Diego, La Jolla, California 92093, USA*
[3]*Institute for Experimental and Applied Physics, Kiel University, 24098 Kiel, Germany*
[4]*LCLS, SLAC National Accelerator Laboratory, Menlo Park, California 94025, USA*
[5]*Ruprecht Haensel Laboratory, Kiel University, 24098 Kiel, Germany*
(Received 20 March 2016; published 25 July 2016)

Symmetry breaking and the emergence of order is one of the most fascinating phenomena in condensed matter physics. It leads to a plethora of intriguing ground states found in antiferromagnets, Mott insulators, superconductors, and density-wave systems. Exploiting states of matter far from equilibrium can provide even more striking routes to symmetry-lowered, ordered states. Here, we demonstrate for the case of elemental chromium that moderate ultrafast photoexcitation can transiently enhance the charge-density-wave (CDW) amplitude by up to 30% above its equilibrium value, while strong excitations lead to an oscillating, large-amplitude CDW state that persists above the equilibrium transition temperature. Both effects result from dynamic electron-phonon interactions, providing an efficient mechanism to selectively transform a broad excitation of the electronic order into a well-defined, long-lived coherent lattice vibration. This mechanism may be exploited to transiently enhance order parameters in other systems with coupled degrees of freedom.

The coupling between various degrees of freedom drives the formation of complex orders in strongly correlated electron systems [1,2]. For instance, charge-lattice coupling creates charge-density-wave (CDW) order [3,4], while more intricate spin-charge-orbital-lattice coupling leads to combined charge and orbital order in manganites [5,6] or charge-spin stripe order in cuprates [2]. Recent studies suggest that spin order can be generated in iron pnictides in response to excitation of a coherent phonon [7], charge localization can be photoinduced in charge order systems [8], the superconducting order parameter in cuprates can be enhanced via suppression of the competing charge order or the transient redistribution of superconducting coherence [9–11], and hidden electronic states can be dynamically accessed [12–15]. Here we demonstrate a dramatic transient enhancement of the CDW amplitude in elemental chromium (Cr) following photoexcitation. This is remarkable, because external excitation typically creates disorder, reduces the order parameter, and raises the symmetry [16–19]. We attribute the enhancement of the CDW amplitude to the dynamic electron-phonon interaction and experimentally discern multiple time scales, thus revealing the underlying physics.

The system we studied is a crystalline Cr film, which is antiferromagnetic and exhibits an incommensurate spin-density wave (SDW) below the Néel temperature $T_N = 290 \pm 5$ K. It also forms an incommensurate CDW, appearing as the second harmonic of the fundamental SDW ordering [3] [see Figs. 1(a) and 1(b)]. The amplitude

of the CDW can be directly measured by x-ray diffraction as the intensity of the corresponding satellite peaks. X rays are mostly sensitive to the core electrons, and the quantity we observe in our experiment is the elastic component of the CDW (periodic lattice distortion). Static x-ray data are presented in Fig. 1(c) and reveal that the CDW has a wave vector normal to the film surface, is pinned by the film surfaces, and is quantized with 8.5 periods in the film, as expected from earlier studies [3,20,21]. Here, the satellite peaks form constructive and destructive x-ray interference with the Laue oscillations, which leads to an increase of the scattered intensity at $[0, 0, 2 - 2\delta]$ or decrease at $[0, 0, 2 + 2\delta]$ [22,23] (2δ being the momentum transfer of the CDW). We used short optical laser pulses to excite ultrafast dynamics in the Cr thin film, and the time-dependent CDW amplitude was monitored via ultrafast x-ray diffraction [insets in Fig. 1(c)]. The experiment was conducted at the x-ray free-electron laser at the Linac Coherent Light Source (LCLS) facility [26,27] in the stroboscopic mode. The sample thickness was 28 nm, the optical (x-ray) pulses had a wavelength of 800 nm (0.14 nm) and a pulse duration of 40 fs (15 fs), and the initial sample temperature was 115 K [23].

The time-dependent x-ray diffraction signal of the CDW satellite peak at $q = 2 - 2\delta$ is shown in Fig. 2 and reveals oscillations following photoexcitation (see [23] for Supplemental movies). The remarkable quality of the data allows unambiguous detection of four different time scales.
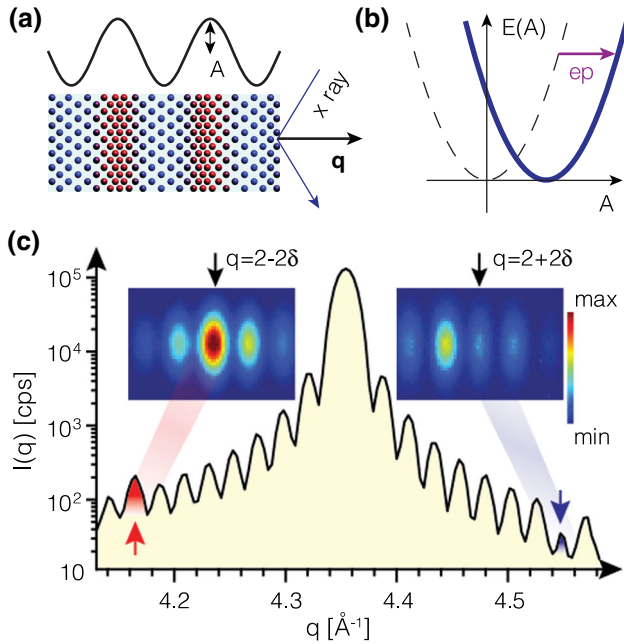
(a)

(b)

(c)

FIG. 1.   Static x-ray diffraction data. (a) Schematic real space representation of the atomic positions in Cr in the presence of a CDW. The corresponding charge density modulation with the CDW amplitude A and the scattering geometry are also shown. (b) The potential energy surface for the CDW amplitude A. In the low-temperature ground state, the potential energy surface is shifted towards a nonvanishing value due to the electron-phonon (ep) coupling. (c) X-ray diffraction from a Cr thin film recorded with synchrotron radiation around the (002) Bragg peak (in photons per second) measured at a film temperature of 115 K. The intensity is increased (reduced) at the positions of the CDW satellites for low (high) q values (indicated by arrows). Insets: Diffraction patterns (linear scale) collected with the x-ray free-electron laser at two different momentum transfers $q = 2 - 2\delta$ and $q = 2 + 2\delta$ in the ground state, corresponding to different incident angles of x rays.

The main oscillation has a period of 453 ± 1 fs and is damped with a time constant of 3.0 ± 0.5 ps so that about 20 oscillations are observed. Strikingly, for low pump fluences the mean of the oscillation increases rapidly in less than 0.5 ps, whereas for higher fluences it remains fixed at 0 [Fig. 2(b)]. The CDW diffraction signal after significant damping of the oscillation (10 ps) decreases with pump fluence and reaches a value of 0 at 11 mJ/cm². At $q = 2 + 2\delta$, an identically opposite behavior occurs due to destructive interference [23] [see Fig. 2(b)]. A positional shift of the Laue oscillations is observed for high fluences and shows a period of 8 ps [see Fig. 2(a)]. This shift is initiated by the temperature increase of the lattice and is used to calibrate the film temperature [23]. In the following, we describe the physical processes that occur on shorter time scales.

The x-ray data measured at specific time delays within the first 0.5 ps are presented in Fig. 3, and the respective time-dependent CDW is schematically depicted in the insets in Fig. 3(a). In the low-temperature equilibrium state

(negative time delay), the x-ray data are consistent with the presence of the CDW nodes at both interfaces [22]. At a time delay of 0.11 ps after photoexcitation, the dynamic x-ray data are in agreement with static x-ray data recorded above the Néel temperature T_N and show an undistorted lattice. At 0.22 ps, we observed a reversal of the CDW amplitude, as revealed by the change of sign of the interference term in the diffraction signal [22,23]. The CDW still has nodes at the interfaces; however, the amplitude is inverted. The most striking observation of our study is the transient enhancement of the CDW amplitude at a time delay of 0.45 ps following moderate laser excitation [Figs. 2(b) and 3]. The transient enhancement is oscillatory and occurs up to a time delay of 4 ps.

The fluence dependence of the pump-probe data reveals that the CDW amplitude is enhanced by about 30% above the maximum value in equilibrium at a fluence of 1 mJ/cm² [see Figs. 4(a)–4(c)]. The experimental observation of the CDW amplitude enhancement was recorded in several independent measurements: the time traces for different fluences (Fig. 2), the fluence dependence of the dynamic CDW amplitude [Figs. 4(a)–4(c)], and in the measurements of both satellite peaks at $q = 2 - 2\delta$ and $q = 2 + 2\delta$ [23]. To exclude the possibility of exciting a broad phonon spectrum [28,29], we measured the transient signal at multiple q values [23]. Only at the position of the satellite peak do we see an oscillation of the scattering intensity. This demonstrates that for low fluences no significantly excited lattice vibrations occur, apart from the CDW, and that the enhancement of the CDW amplitude is due to the preexisting CDW in the film.

We attribute the enhancement of the CDW amplitude to dynamic electron-phonon interaction and present a model for the underlying physical processes in Fig. 4(d). The model is corroborated by fits to the data based on the theory of displacive excitation of coherent phonons [23,30–32]. We start with the low-temperature ground state [see Fig. 4(d), $\tau < 0$ ps], where the electronic order and electron-phonon coupling are responsible for the presence of the static CDW [3]. The schematic potential energy surface (blue curve) for the CDW amplitude, A, is centered at $A_0 > 0$, its value in the low-temperature ground state [see also Fig. 1(b)].

The photoexcitation creates hot charge carriers with temperatures well above T_N within less than 50 fs [23,33], the electronic order is partially suppressed, and the electronic and lattice degrees of freedom are partially decoupled [see Fig. 4(d), $\tau \sim 0$ ps]. The lattice distortion is still frozen; however, the potential energy surface has a new transient minimum at A_1 (red dashed curve) with a smaller or vanishing mean CDW amplitude due to the quenched electronic order. The lattice mode is thus released and starts oscillating. The frequency of this coherent lattice oscillation ($\nu = 2.21$ THz) is in agreement with the frequency of the longitudinal acoustic phonon at the corresponding wavelength measured in bulk chromium [34]. The initial drop of
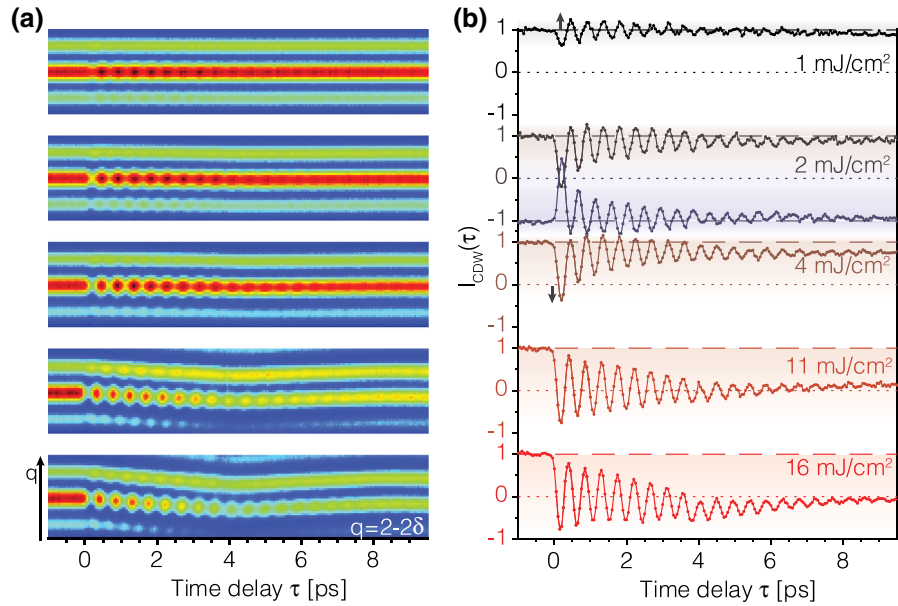
FIG. 2.   Time resolved x-ray diffraction data. (a) Time dependence of the intensity in the vicinity of the CDW satellite at $q = 2 - 2\delta$ (see Fig. 1) for a series of pump fluences (incident, p polarization). (b) The black and red lines show the normalized transient intensity difference $\Delta I_{\mathrm{CDW}}(\tau) = [I_{\mathrm{CDW}}(\tau) - I_{\mathrm{RT}}]/|I_{\mathrm{CDW},0} - I_{\mathrm{RT}}|$ at $q = 2 - 2\delta$, where I_{CDW} is the data in (a), I_{RT} was measured at room temperature above T_N without CDW, and $I_{\mathrm{CDW},0}$ was measured in the low-temperature ground state. The intensity difference rises above its initial value of one for low fluences and drops below zero as the fluence increases (indicated by arrows). The blue line shows $\Delta I_{\mathrm{CDW}}(\tau)$ at $q = 2 + 2\delta$ for a fluence of 2 mJ/cm^2 and starts at -1 due to destructive interference.

the CDW amplitude after 0.22 ps saturates at a fluence of 4 mJ/cm^2 [Fig. 4(c)], and A does not decrease below a value of -0.9. Therefore, the amplitude $A_1 = 0$ in Fig. 4(d) limits the initial displacement of the potential energy surface, indicating that only the preloaded energy due to the frozen phonon is released via quenching of the electronic order.

Surprisingly, for low fluences (smaller than 4 mJ/cm^2), we observe a dramatic deviation from the conventional model for displacive excitation of coherent phonons: here, the minimum of the potential energy surface rapidly shifts back towards the initial ground state A_0 [see Fig. 4(d), $\tau \sim t_{\mathrm{ep}}$] [35]. To reproduce this essential feature of our data, we added a superimposed exponential relaxation of the displacive component to the fit [23]. The time constant for this relaxation was determined to be 300 fs, in good agreement with the carrier-lattice thermalization time measured by optical reflectivity [33]. Therefore, our analysis indicates that while the carriers cool down below T_N the electronic ordering is reestablished and pulls the quasiequilibrium minimum of the potential energy surface towards higher values. In other words, the electronic and the lattice degrees of freedom recouple within less than 0.5 ps. This ultrafast backshift and the weak damping of the lattice oscillations about the dynamic quasiequilibrium are the essence of the transient enhancement of the CDW amplitude [see Fig. 4(d), $\tau > t_{\mathrm{ep}}$]. The enhancement at 0.45 ps is maximized at a fluence of 1.2 mJ/cm^2 [see the vertical dashed line in Fig. 4(c)], which is coincident with the zero crossing of the CDW amplitude at 0.22 ps and

indicates lattice-assisted recondensation of the electronic ordering.

The relaxation time slightly increases with pump fluence, which is qualitatively supported by calculations within the two-temperature model [23,33,36–38]; i.e., for increased fluences the carrier temperature stays longer above T_N. At even higher fluences (larger than 11 mJ/cm^2), when the quasiequilibrium temperature after carrier-lattice equilibration approaches or exceeds T_N, no shift of the potential energy surface occurs and the CDW amplitude oscillates around zero, the value it would assume in equilibrium above T_N [Fig. 2(b)]. Since damping is also remarkably weak in the strong excitation regime, the CDW amplitude oscillations can persist above T_N. It is worth noting that the data measured with 1 mJ/cm^2 in Fig. 2(b) could be interpreted in terms of an impulsive excitation of the coherent phonon mode, i.e., excitation without displacement of the potential energy surface, whose characteristic signature is a sine-type oscillatory behavior [39]. The high fluence data (larger than 11 mJ/cm^2), however, clearly show that the coherent phonon is driven by a displacive excitation (cosine-type behavior). The correct interpretation relies on the dynamical picture introduced in Fig. 4(d), and the reforming of the electronic ordering is indispensable in explaining the CDW amplitude enhancement, because the amplitude of the lattice oscillation is always smaller than the initial suppression of the mean value (see Table S1).

The damping time constant of the coherent lattice oscillation is about 3 ps and independent of the fluence.
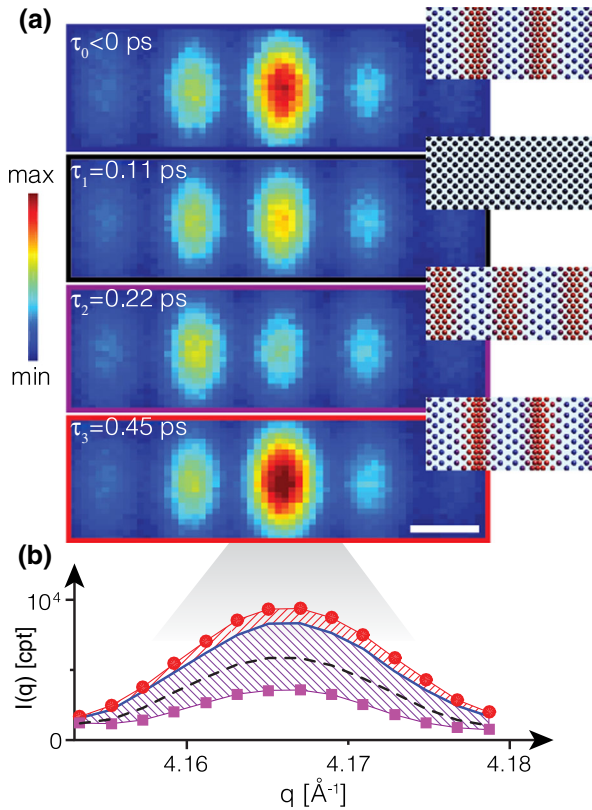
FIG. 3. Interpretation of the time resolved x-ray diffraction data. (a),(b) X-ray data around $q = 2 - 2\delta$ (a) and the integral along the vertical direction (b) in photons per second recorded at time delays τ_0 before 0 ps (blue solid line), $\tau_1 = 0.11$ ps (black dashed line, 5 mJ/cm^2), $\tau_2 = 0.22$ ps (magenta squares, 5 mJ/cm^2), and $\tau_3 = 0.45$ ps (red circles, 1 mJ/cm^2). The time delays represent significant instants in the first period of the oscillation in Fig. 2. Insets in (a): Schematic representations of the charge density modulation that are consistent with the x-ray data for different time delays. The charge density at 0.11 ps is similar to the room temperature case, where no CDW is present. The scale bar in (a) shows 0.025 Å^{-1}.

This surprisingly long time scale indicates anharmonic phonon-phonon interaction as the dominant decay channel. Electron-hole pair excitation, which typically leads to strong damping of order-parameter oscillations in strongly correlated electron systems [32,40,41], is expected to be ineffective here because of the SDW gap in the electronic spectrum [42]. Because of ultrafast carrier cooling and recondensation in the lattice distortion potential, this gap will quickly reopen, even after a complete quench of the electronic order [17]. Moreover, it is likely to persist above T_N in the form of a pseudogap due to incipient magnetic order [42]. Finally, the period of the lattice oscillation is much shorter than the damping time and also does not depend on fluence [23]. Thus, the Cr system studied here essentially represents an effective converter of an electronic excitation into a well-defined, long-lived CDW amplitude oscillation: an oscillation that leads to a significant transient
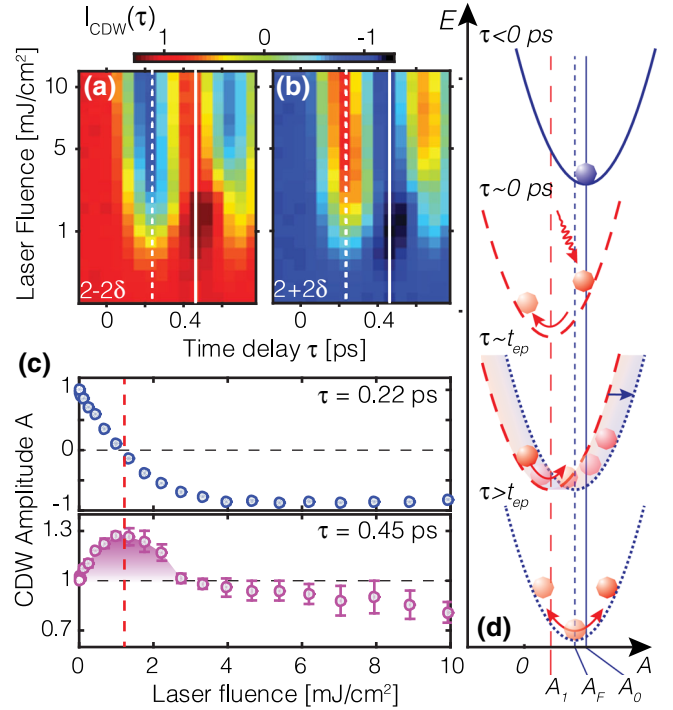
FIG. 4. Enhancement of the CDW amplitude. (a),(b) The normalized intensity of the CDW satellite peak (see the caption of Fig. 2) as a function of the pump fluence and time delay for $q = 2 - 2\delta$ (a) and $q = 2 + 2\delta$ (b). (c) The transient amplitude of the CDW at 0.22 ps (top, first minimum of the oscillation in Fig. 2) and 0.45 ps (bottom, first maximum of the oscillation in Fig. 2) extracted as line scans along the white lines in (a) and (b). (d) A schematic illustration of the mechanism behind the enhancement of the CDW amplitude due to dynamic electron-phonon interaction. The potential energy surfaces are drawn for the dynamic CDW amplitude, shown on the horizontal axis. A_0 is the amplitude of the CDW in the ground state, A_1 is the quasiequilibrium position after the excitation, and A_F is its position after 10 ps. The transient amplitude $A(\tau)$ was fitted by the following equation $A(\tau) = A_F + B\cos(2\pi\tau'/\tau_P)\exp(-\tau'/\tau_D) - C\exp(-\tau'/\tau_{ep})$, where B is the amplitude, τ_P the period, and τ_D the damping time of the oscillation, $\tau' = \tau - \tau_0$, τ_0 is the offset of the oscillation, $C = A_F - A_1$, and t_{ep} is the decay time for the shift of the quasiequilibrium towards A_F [23].

enhancement of the CDW amplitude and that can even persist above the equilibrium transition temperature. We anticipate that other sorts of excitation would lead to a similarly well-defined and persistent oscillation of the CDW amplitude in this system.

In summary, by using the unique capabilities now possible with the hard x-ray free-electron lasers, we directly observe a dramatic enhancement of the CDW amplitude in chromium following photoexcitation: 30% above its maximum value in equilibrium. We identify the ultrafast underlying physical processes by discerning multiple time scales and explain our results by three main processes, referred to as "dynamic electron-phonon interaction" throughout the

Letter: (i) the photoinduced quench of the electronic order unfreezes a coherent lattice oscillation, (ii) the mean amplitude of this lattice oscillation is increased due to the ultrafast recondensation of the electronic order, and (iii) the reordering of electrons is assisted by the still present lattice distortion. The rapid electronic recondensation is evident from both the ultrafast backshift of the mean of the oscillation and the weak damping of the oscillation due to the reopening of the electronic gap. A further interesting question is whether the dynamic electron-phonon interaction can be combined with repeated photoexcitation to maintain the coherent lattice oscillation or to achieve an even higher enhancement of the CDW amplitude [43,44]. Our results also raise fundamental questions regarding the dynamics of the magnetic ordering and the electronic structure of the system. Finally, we anticipate that the enhancement of an order parameter via dynamic interaction of various degrees of freedom is a general phenomenon and can be observed and studied both theoretically and experimentally in a variety of systems including topological insulators [45] and strongly correlated electron materials [8].

*Corresponding author.
ansinger@ucsd.edu
†Present address: Paul Scherrer Institut, CH-5232 Villigen, Switzerland.

[1] M. Imada, A. Fujimori, and Y. Tokura, Rev. Mod. Phys. **70**, 1039 (1998).
[2] E. Dagotto, Science **309**, 257 (2005).
[3] E. Fawcett, Rev. Mod. Phys. **60**, 209 (1988).
[4] G. Gruner, *Density Waves in Solids* (Perseus, Cambridge, England, 2009).
[5] J. van den Brink, G. Khaliullin, and D. Khomskii, Phys. Rev. Lett. **83**, 5118 (1999).
[6] E. Dagotto, New J. Phys. **7**, 67 (2005).
[7] K. W. Kim, A. Pashkin, H. Schäfer, M. Beyer, M. Porer, T. Wolf, C. Bernhard, J. Demsar, R. Huber, and A. Leitenstorfer, Nat. Mater. **11**, 497 (2012).
[8] T. Ishikawa, Y. Sagae, Y. Naitoh, Y. Kawakami, H. Itoh, K. Yamamoto, K. Yakushi, H. Kishida, T. Sasaki, S. Ishihara, Y. Tanaka, K. Yonemitsu, and S. Iwai, Nat. Commun. **5**, 5528 (2014).

[9] D. Fausti, R. I. Tobey, N. Dean, S. Kaiser, A. Dienst, M. C. Hoffmann, S. Pyon, T. Takayama, H. Takagi, and A. Cavalleri, Science **331**, 189 (2011).
[10] R. Mankowsky, A. Subedi, M. Först, S. O. Mariager, M. Chollet, H. T. Lemke, J. S. Robinson, J. M. Glownia, M. P. Minitti, A. Frano, M. Fechner, N. A. Spaldin, T. Loew, B. Keimer, A. Georges, and A. Cavalleri, Nature (London) **516**, 71 (2014).
[11] W. Hu, S. Kaiser, D. Nicoletti, C. R. Hunt, I. Gierz, M. C. Hoffmann, M. Le Tacon, T. Loew, B. Keimer, and A. Cavalleri, Nat. Mater. **13**, 705 (2014).
[12] K. Onda, S. Ogihara, K. Yonemitsu, N. Maeshima, T. Ishikawa, Y. Okimoto, X. Shao, Y. Nakano, H. Yamochi, G. Saito, and S.-Y. Koshihara, Phys. Rev. Lett. **101**, 067403 (2008).
[13] H. Ichikawa, S. Nozawa, T. Sato, A. Tomita, K. Ichiyanagi, M. Chollet, L. Guerin, N. Dean, A. Cavalleri, S. Adachi, T. Arima, H. Sawa, Y. Ogimoto, M. Nakamura, R. Tamaki, K. Miyano, and S. Koshihara, Nat. Mater. **10**, 101 (2011).
[14] L. Stojchevska, I. Vaskivskyi, T. Mertelj, P. Kusar, D. Svetin, S. Brazovskii, and D. Mihailovic, Science **344**, 177 (2014).
[15] V. R. Morrison, R. P. Chatelain, K. L. Tiwari, A. Hendaoui, A. Bruhács, M. Chaker, and B. J. Siwick, Science **346**, 445 (2014).
[16] F. Schmitt, P. S. Kirchmann, U. Bovensiepen, R. G. Moore, L. Rettig, M. Krenz, J.-H. Chu, N. Ru, L. Perfetti, D. H. Lu, M. Wolf, I. R. Fisher, and Z.-X. Shen, Science **321**, 1649 (2008).
[17] A. Tomeljak, H. Schäfer, D. Städter, M. Beyer, K. Biljakovic, and J. Demsar, Phys. Rev. Lett. **102**, 066404 (2009).
[18] M. Eichberger, H. Schäfer, M. Krumova, M. Beyer, J. Demsar, H. Berger, G. Moriena, G. Sciaini, and R. J. D. Miller, Nature (London) **468**, 799 (2010).
[19] P. Beaud et al., Nat. Mater. **13**, 923 (2014).
[20] H. Zabel, J. Phys. Condens. Matter **11**, 9303 (1999).
[21] E. E. Fullerton, J. L. Robertson, A. R. E. Prinsloo, H. L. Alberts, and S. D. Bader, Phys. Rev. Lett. **91**, 237201 (2003).
[22] A. Singer, M. J. Marsh, S. H. Dietze, V. Uhlíř, Y. Li, D. A. Walko, E. M. Dufresne, G. Srajer, M. P. Cosgriff, P. G. Evans, E. E. Fullerton, and O. G. Shpyrko, Phys. Rev. B **91**, 115134 (2015).
[23] See Supplemental Material at http://link.aps.org/supplemental/10.1103/PhysRevLett.117.056401 for supplementary movies, further experimental details, calculation of the CDW amplitude from the satellite peak intensity, data at $q = 2 + 2\delta$, details on x-ray data analysis, calculation of the fluence, calculation of the temperature, measurements at multiple q-values, Fourier spectra of the time traces, and fit details and results, which includes Refs. [24,25].
[24] S. Friedberg, I. Estermann, and J. Goldman, Phys. Rev. **85**, 375 (1952).
[25] C. Kittel, *Introduction to Solid State Physics* (Wiley, New York, 1953).
[26] P. Emma et al., Nat. Photonics **4**, 641 (2010).
[27] D. Zhu, Y. Feng, S. Stoupin, S. A. Terentyev, H. T. Lemke, D. M. Fritz, M. Chollet, J. M. Glownia, R. Alonso-Mori, M. Sikorski, S. Song, T. B. van Driel, G. J. Williams, M.

Messerschmidt, S. Boutet, V. D. Blank, Y. V. Shvyd'ko, and A. Robert, Rev. Sci. Instrum. **85**, 063106 (2014).

[28] M. Trigo *et al.*, Nat. Phys. **9**, 790 (2013).

[29] D. Zhu, A. Robert, T. Henighan, H. T. Lemke, M. Chollet, J. M. Glownia, D. A. Reis, and M. Trigo, Phys. Rev. B **92**, 054303 (2015).

[30] H. J. Zeiger, J. Vidal, T. K. Cheng, E. P. Ippen, G. Dresselhaus, and M. S. Dresselhaus, Phys. Rev. B **45**, 768 (1992).

[31] A. Melnikov, I. Radu, A. Povolotskiy, T. Wehling, A. Lichtenstein, and U. Bovensiepen, J. Phys. D **41**, 164004 (2008).

[32] T. Huber, S. O. Mariager, A. Ferrer, H. Schäfer, J. A. Johnson, S. Grübel, A. Lübcke, L. Huber, T. Kubacka, C. Dornes, C. Laulhe, S. Ravy, G. Ingold, P. Beaud, J. Demsar, and S. L. Johnson, Phys. Rev. Lett. **113**, 026401 (2014).

[33] S. D. Brorson, A. Kazeroonian, J. S. Moodera, D. W. Face, T. K. Cheng, E. P. Ippen, M. S. Dresselhaus, and G. Dresselhaus, Phys. Rev. Lett. **64**, 2172 (1990).

[34] W. Shaw and L. Muhlestein, Phys. Rev. B **4**, 969 (1971).

[35] The potential minimum does not reach its initial value A_0 owing to the increase of the film temperature.

[36] S. I. Anisimov, B. L. Kapeliovich, and T. L. Perel'man, Zh. Eksp. Teor. Fiz. **66**, 776 (1974) [Sov. Phys. JETP **39**, 375 (1974)].

[37] R. H. M. Groeneveld, R. Sprik, and A. Lagendijk, Phys. Rev. B **51**, 11433 (1995).

[38] The same qualitative result is obtained in the more sophisticated nonthermal electron model where the electron relaxation time is fluence independent, and for increased fluences the carrier temperature remains longer above T_N because of the higher initial rise.

[39] K. Ishioka and O. K. Misochko, *Progress in Ultrafast Intense Laser Science* (Springer, Berlin, 2010).

[40] P. Beaud, S. L. Johnson, A. Streun, R. Abela, D. Abramsohn, D. Grolimund, F. Krasniqi, T. Schmidt, V. Schlott, and G. Ingold, Phys. Rev. Lett. **99**, 174801 (2007).

[41] H. Schaefer, V. V. Kabanov, and J. Demsar, Phys. Rev. B **89**, 045106 (2014).

[42] R. Jaramillo, Y. Feng, J. C. Lang, Z. Islam, G. Srajer, H. M. Rønnow, P. B. Littlewood, and T. F. Rosenbaum, Phys. Rev. B **77**, 184418 (2008).

[43] T. Onozaki, Y. Toda, S. Tanda, and R. Morita, Jpn. J. Appl. Phys. **46**, 870 (2007).

[44] P. Kusar, T. Mertelj, V. V. Kabanov, J.-H. Chu, I. R. Fisher, H. Berger, L. Forró, and D. Mihailovic, Phys. Rev. B **83**, 035104 (2011).

[45] I. Garate, Phys. Rev. Lett. **110**, 046402 (2013).